Biochimica et Biophysica Acta, 509 (1978) 300—317

BBA 78021

TRANSIENT PHOTOVOLTAGES IN PURPLE MEMBRANE MULTILAYERS

CHARGE DISPLACEMENT IN BACTERIORHODOPSIN AND ITS PHOTOINTERMEDIATES

SAN-BAO HWANG [a], JUAN I. KORENBROT [a,*] and WALTHER STOECKENIUS [b]

[a] *Departments of Physiology and Biochemistry and* [b] *The Cardiovacular Research Institute, University of California School of Medicine, San Francisco, Calif. 94143 (U.S.A.)*

(Received November 7th, 1977)

Summary

The photovoltaic properties of bacteriorhodopsin molecules and their photochemical intermediates have been investigated in an experimental cell consisting of multilayered films of highly oriented, dry fragments of purple membrane and lipid sandwiched between two metal (Pd) electrodes. The electrical time constant of these sandwich cells containing between 5 and 30 layers is $<10^{-6}$ s. Bright illumination of these cells with actinic flashes of $\approx$1 ms duration generates transient photovoltages. These photovoltages, which make the extracellular surface of purple membrane positive with respect to the intracellular surface, follow the time course of the flash with no detectable latency. The amplitude of the photovoltages increases linearly with light intensity and their action spectrum matches the absorption spectrum of the light-adapted state of bacteriorhodopsin, BR_{570}. In these dry multilayer cells, the slow photointermediates of bacteriorhodopsin, M_{412}, N_{520} and O_{640} are long lived. Illumination of the sandwhich cells with long duration (200 ms) pulses of light results, therefore, in the formation of photomixtures containing all these slow photointermediates. Flash illumination of the sandwich cells immediately following the conditioning pulse produces photovoltages whose action spectra match the absorption spectra of the M_{412} and N_{520} photointermediates. The M_{412} photovoltages, like the BR_{570} photovoltages, follow the time course of the actinic flash with no detectable latency and increase in amplitude linearly with light intensity. But, unlike the BR_{570} photovoltage, the M_{412}, N_{520} and O_{640} photovoltages make the extracellular surface of purple membrane negative with respect to the intracellular surface. Through the use of their specific photovoltaic signals, M_{412} and N_{520} are shown to be kinetically distinct photointermediates of bacteriorhodopsin. Detection of fast photo-

* To whom correspondence should be addressed.

voltages with these characteristics in the absence of any ionic solution, and in parallel with spectrophotometric changes, suggest that they arise from charge displacements in the bacteriorhodopsin molecules and their photointermediates as they undergo photochemical conversion in response to the absorption of photons.

Introduction

Bacteriorhodopsin is a light-absorbing protein embedded within structurally distinct areas of the plasma membrane of *Halobacterium halobium* known as "purple membrane" [1]. Bacteriorhodopsin molecules constitute the only protein component of the purple membrane [1,2] and function as light-driven proton pumps [3,4]. Each bacteriorhodopsin molecule contains a single retinal chromophore covalently bound through a Schiff base [1,2]. Protonation of this Schiff base [5,6] and non-covalent interaction between chromophore and protein [7,8] result in the characteristic visible absorption spectrum of bacteriorhodopsin which consists of a single broad band with 570 nm λ_{max} in the light-adapted state (BR_{570}) [1,9]. Upon absorption of light, bacteriorhodopsin molecules proceed through a cyclic sequence of at least five different photochemical intermediates [9—12]. Each of these photointermediates is characterized by a distinct visible absorption spectrum and Lozier et al. [9] have designated them, according to their temporal sequence and wavelength of maximum absorbance as K_{590}, L_{550}, M_{412}, N_{520} and O_{640}. The initial conversion of BR_{570} into K_{590} is the only step which requires light [9]. The K_{590} intermediate decays thermally in the dark through the sequence L_{550}, M_{412}, N_{520} and O_{640}, and the rate of these transitions is hence a function of temperature [9,11,13—15]. Only at temperatures above —50°C is the sequence of intermediates cyclic, finally returning to the BR_{570} state. The rates of thermal conversion between photointermediates have also been found to depend on other parameters, such as the isotopic form of hydrogen present in solution [13,14], the pH [15] and the ionic composition of the solution [12]. In dry samples of purple membrane, these rates are slower than in aqueous suspensions [16]. At room temperature and physiological pH, the half-time of the photoreaction cycle in an aqueous suspension of purple membrane is about 10 ms [17].

In the course of each photoreaction cycle, bacteriorhodopsin molecules first release protons on the extracellular surface of the purple membrane and then take them up on the intracellular surface [17—19]. In aqueous suspensions of purple membrane the proton release occurs shortly after the formation of the M_{412} intermediate and the uptake occurs with the appearance of O_{640} or BR_{570} [17]. The mechanism of this proton translocation by bacteriorhodopsin in the light remains unknown. This proton transport, however, is known to be electrogenic and results, thus, in the generation of photovoltages which have been measured in intact bacteria [20,21], bacterial cell membrane envelopes [22] and model systems into which purple membrane fragments are incorporated [23—25,19]. These photovoltages exhibit an action spectrum which matches the absorption spectrum of BR_{570} and are linearly proportional to light intensity only at low stimulus intensity, becoming non-linear at high

intensities [19]. Since these photovoltages arise from a transmembrane flux of protons, they develop slowly, have a latency with respect to the presentation of the light stimulus and result exclusively in the extracellular surface of the purple membrane becoming positive with respect to the intracellular surface [21,22,19]. In contrast to these photovoltages, Trissl and Montal [26] have suggested that photoexcitation of BR_{570} can also generate capacitative photovoltages which reflect conformational changes in the protein molecule. The study of such photovoltaic properties of the bacteriorhodopsin molecule may lead to insights into the mechanism of the protein function.

The photovoltaic properties of biological molecules such as chlorophyll [27] and of organic molecules such as tetracene [28] have been extensively studied in the past with the use of experimental cells consisting of oriented films of these molecules sandwiched between metal electrodes. To study the photovoltaic properties of bacteriorhodopsin we have constructed similar cells consisting of dried multilayers of air-water interface films of oriented purple membrane and lipid, which we have described previously [16,19], sandwiched between palladium (Pd) electrodes. We describe here the electrical properties of these experimental cells and report the measurement of transient photovoltages generated specifically by the photoexcitation of BR_{570} and several of the photointermediates in the photoreaction cycle of bacteriorhodopsin.

Materials and Methods

Materials. Purple membrane fragments from *H. halobium* were isolated and purified as described by Oesterhelt and Stoeckenius [29]. Spectrophotometric grade hexane was obtained from Mallinckrodt (Palo Alto, Calif.) and redistilled in small volumes shortly before use. Palladium wire (100% pure, 0.2 mm diameter) and tungsten wire (0.62 mm diameter) were purchased from Ladd Research Industries, Inc. (Burlington, Vt.). Optically flat pyrex glass was obtained from Edmund Scientific Co. (Barrington, N.J.). All water was glass distilled four times including once from alkaline permanganate and once from sulfuric acid.

Preparation of purple membrane-metal sandwich cell. The model system used in the experiments reported here consisted of a dry multilayer stack of oriented purple membrane fragments and lipid sandwiched between two metal electrodes. The metal electrodes were formed by vacuum deposition of Pd on a flat glass support. A circular glass slide (27 mm diameter, 2 mm thick) was cleaned for 1 h by immersion in a warm dichromate-sulfuric acid solution, it was then rinsed thoroughly with running distilled water and dried under a stream of nitrogen. A thin layer of Pd (30—60% transmittance at 500 nm) of 2.85 cm^2 area was then immediately vapor deposited onto the glass slide under a vacuum of between $1 \cdot 10^{-6}$ and $5 \cdot 10^{-6}$ Torr in a Norton Evaporator (NRC 3117, Norton Vacuum Equipment Division) with tungsten wire as the heating element.

Purple membrane multilayers were formed by repeatedly inserting and withdrawing the Pd covered glass slide across an air-water interface film consisting of oriented purple membrane fragments separated by a lipid monolayer. The purple membrane interface film was formed in a Teflon Langmuir trough by

spreading onto a clean air-water interface a hexane suspension of sonicated purple membrane fragments (0.5 mg protein/ml), prepared as previously described [16], except that no soya phosphatidylcholine was added. In all experiments the subphase was unbuffered water, pH 5.6—5.8. The interface film was brought to its collapse pressure (47 dynes/cm), and maintained at the value during transfer by a servo controlled movable barrier in the Langmuir trough that advanced as material transferred from the interface to the slide. The slide emerged wet and was allowed to thoroughly air dry between successive depositions (20—30 min). The bacteriorhodopsin interface film transferred to the Pd-evaporated glass support only on the upward stroke through the interface. This is most important since it resulted in the formation of multilayer stacks in which the purple membrane fragments remained highly oriented. To complete the metal sandwich cell, a second Pd electrode of 2.85 cm^2 area was vapor deposited on top of the purple membrane multilayer stack. A mask was used such that two metal surfaces had an 0.7 ± 0.07 cm^2 area of overlap (see Fig. 1). The vacuum deposition of the second Pd electrode probably resulted in the irreversible damage of the protein in the top few layers of the sandwich cell.

Electrical measurements. The sandwich cell was secured horizontally on a specially designed stage within an electrically shielded black box. Electrical contact with the Pd metal surface was accomplished through thin phosphor bronze metal shims (0.3 mm thick). The d.c. resistance of the sandwich cells was measured with a voltage clamp circuit which permitted recording of the sandwich cell current in response to applied voltage steps. The capacitance of the cells was measured in collaboration with Dr. S. White with a high precision a.c. impedance bridge of his design and construction [30]. The potential differences between the two Pd electrodes in the dark and during light stimulation were measured with a unity gain high input impedance ($R_{in} > 10^{13}$ Ω) differential amplifier with a recording bandwidth of d.c. to 50 kHz (Model 1090, Wilson Electronics, San Francisco, Calif.). Photovoltage signals were further amplified through a variable gain amplifier with a recording bandwidth of d.c. to 10 kHz (Model 3A3, Tektronics, Inc.), and averaged (Model 1074 signal averager, Nicolet Instruments, Madison, Wisc.). Standard pulses were applied to calibrate the time course and amplitude of the averaged photovoltages. Flashlight switching artifacts were rejected with the use of the signal averager by subtracting from each averaged photovoltage the averaged waveform recorded upon flashing the sandwich cell an equal number of times with the light path to the cell completely blocked. Typically, a total of 64 photoresponses were averaged. Averaged waveforms were stored in digital tape for later analyses. Reproducible data could be recorded from the sandwich cells for up to 4 months after their formation. All experiments were carried out at room temperature (20—22°C) and relative humidity (55—70%).

Photostimulator. Light was delivered exclusively to the area of metal electrode overlap in the sandwich cell and special guards were used to insure that the Pd-phosphor bronze contact points were not illuminated. Two different light stimuli were used: (1) An actinic flash of about 1 ms duration (1/2 amplitude, see Fig. 4) produced by a Strobonar 880 unit (Honeywell, Inc.). This light was delivered from below the sandwich cell through a 1.25 cm

diameter and 50 cm long fiberglass light pipe. (2) Pulses of light of variable duration controlled by a mechanical shutter and produced by a 250 W quartz-iodide source (Leitz-Prado Slide Projector). This light was delivered through a system of lenses to the same area illuminated by the actinic flash, but from the opposite direction. Two one-quarter inch thick infrared absorbing glass filters (Edmund Scientific) were used in each light path. Calibrated neutral density (Balzers), colored glass (Corning Glassworks) and interference filters (Baird-Atomic, 15 nm half bandwidth) controlled the wavelength and intensity of the light stimuli, as needed. The power density of the light pulses was measured at the position of the sandwich model cell with a Kettering Radiometer (Model 68, Laboratory Data Control Division). The light energy of the actinic flash was measured with an integrating radiometer (Optometer 40A, United Detector Technology, Santa Monica, Calif.).

Results

In previous communications we have reported in detail on the formation and the structural and functional properties of the air-water interface films used in the present experiments. These films consist of a lipid monolayer containing randomly distributed small fragments of purple membrane which occupy 30—40% of the aqueous surface [16]. Under the experimental conditions reported here, some membrane overlap occurs on the water surface. About 85% of the membrane fragments are oriented at the interface with their intracellular surface towards the aqueous subphase [16]. The bacteriorhodopsin molecules in the membrane fragments at the interface function as light-driven proton pumps [19]. In multilayer stacks of these films we have further shown that bacteriorhodopsin undergoes both its dark-light adaptation reaction and its photoreaction cycle [16].

Stacks of up to 30 successive layers of purple membrane interface film can be built on the Pd-covered glass support. As described under Materials and Methods, the purple membrane film transfers onto the support only during the upward movement of the support through the interface. Because the purple membrane fragments themselves have a preferred orientation at the interface, repetition of this asymmetric transfer yields multilayer stacks in which most of the purple membrane fragments are oriented with their intracellular surface towards the Pd electrode nearest the glass support. Most importantly, these features of orientation of the membrane fragments indicate that the majority of the bacteriorhodopsin molecules in each layer of the stack are electrically in parallel with each other.

Passive electrical properties of the purple membrane sandwich cell

In the dark, the d.c. resistance of all sandwich cells tested ranged from 500 to 2000 $\Omega \cdot cm^2$. All cells tested, consisting of stacks of 5—30 interface layers exhibited these consistently low values of electrical resistance and no evidence of a dependence of resistance on the number of layers in the stack was found. In addition, as shown in Fig. 1, the current-voltage characteristics of the cells are linear to ±150 mV. The capacitance of the sandwich cell was measured to be less than 1 nF/cm^2 at 1000 Hz (this limit is set by the test instrument)

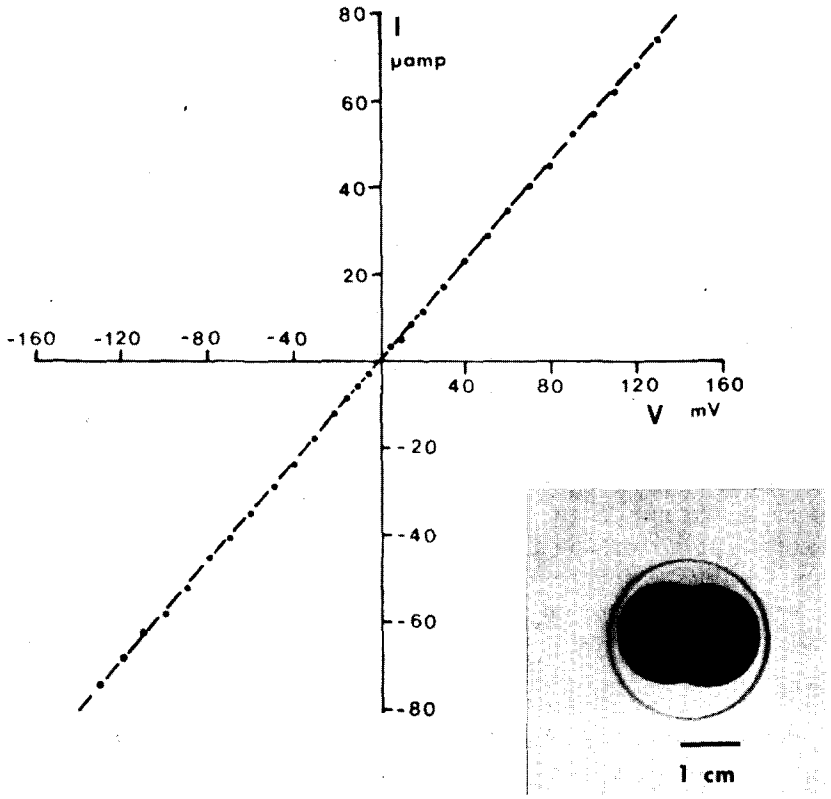

Fig. 1. Current-voltage characteristics of the purple membrane-metal sandwich cell. The sandwich cell consisted of 29 layers sandwiched between Pd electrodes. The current-voltage curve was linear over the range tested. Each point represents the average of three separate measurements. In the lower right quadrant is a photograph of a sandwich cell assembly similar to all other experimental cells used in the present experiments. The area of electrode overlap is 0.7 cm^2.

regardless of the number of layers in the assembly. These data contrast with the resistance of the order of $10^8\ \Omega \cdot cm^2$ reported for monolayers of fatty acids [31] or bilayers of phospholipids [32] sandwiched between metal electrodes. However, to obtain these high resistances, the initially low resistance layers must be thoroughly dried under vacuum or over silica gel for prolonged periods of time. Moreover, Rosenberg and Jendrasiak [33] have shown that the conductivity of vacuum-dried lecithin films increase by 9—11 orders of magnitude when exposed to ambient humidity (see also ref. 34). The electrical properties of the purple membrane sandwich cells, therefore, almost certainly reflect the presence of water in the sandwich cells which are only air dried and are tested at room relative humidity. In any event, the measured values of resistance and capacitance show that the electrical time constant "τ" of the purple membrane sandwich cells is $<10^{-6}$ s for stacks of up to 30 layers. This is a unique experimental advantage in photovoltaic studies since it allows us to observe the kinetics of transient voltage events of time course slower than 10^{-5} s undistorted by the low pass characteristics of the purple membrane sandwich cell

assembly. That is, for events slower than 10^{-5} s, the waveform of the voltage recorded is a measure of the time course of flow of charge.

The BR_{570} photovoltage

In the dark, there is no voltage difference between the two Pd electrodes in the purple membrane sandwich cells. In contrast, when the cell assembly is illuminated with brief actinic flashes, transient photovoltages are recorded such as those shown in Fig. 2. The polarity of these photovoltages indicates that the extracellular surface of purple membrane becomes transiently positive with respect to its intracellular surface. As illustrated in Fig. 2, the maximum amplitude of the photovoltages is linearly proportional to the intensity of the stimulus flash, regardless of its color, over the range tested here. The maximum amplitude of the photovoltages, but not their waveform, depends on the stimulus wavelength. Fig. 3 illustrates photovoltages recorded in response to flashes of various wavelengths but identical intensities. Using data such as that shown, it is possible to construct the action spectrum of the photovoltages by plotting the peak signal amplitude of the transient voltage for the different wavelengths tested. The action spectrum thus obtained is shown in Fig. 3. The action spectrum exhibits a single broad band with a λ_{max} near 570 nm which matches very well the absorption spectrum of the light-adapted forms of bacteriorhodopsin, BR_{570}. These results indicate, therefore, that transient photovoltages are produced by a phenomenon closely associated with the photoexcitation of BR_{570} and that the magnitude of the photovoltages are directly proportional to the number of photoexcited pigment molecules.

For all intensities tested and for all wavelengths tested the waveform of the BR_{570} photovoltage is the same, as is shown in Figs. 2 and 3. The waveform of the photovoltage is essentially identical to that of the actinic flash, and it

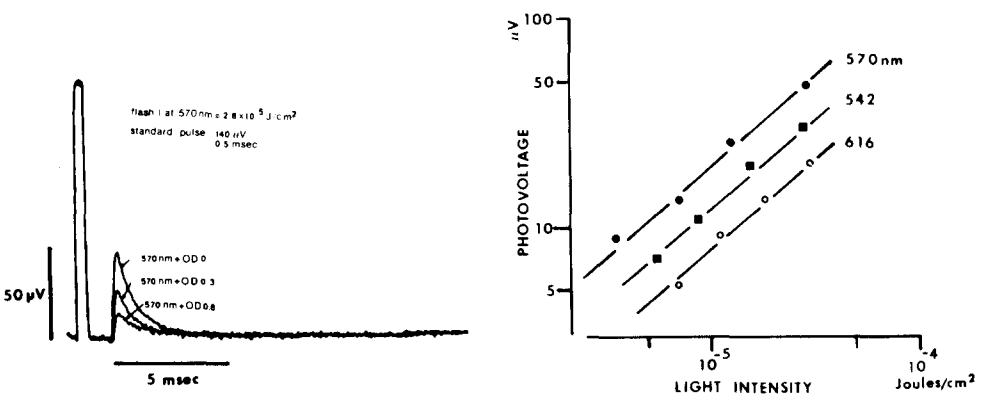

Fig. 2. Light intensity dependence of the BR_{570} photovoltage. Each tracing is the signal average of 64 photoresponses to actinic flashes presented at 20-s intervals. A calibrating standard pulse was also signal averaged. Illustrated are photoresponses to actinic flashes of various intensities presented through a 570 nm narrow band interference filter (15 nm half-band width). The graph illustrates the peak amplitude of photovoltages generated at various intensities for stimuli at three different wavelengths. Under all conditions of photoexcitation tested, the voltage yielded the extracellular surface of the purple membrane transiently positive with respect to the intracellular surface. The data shown were recorded from a multilayer sandwich cell consisting of 17 interface layers.

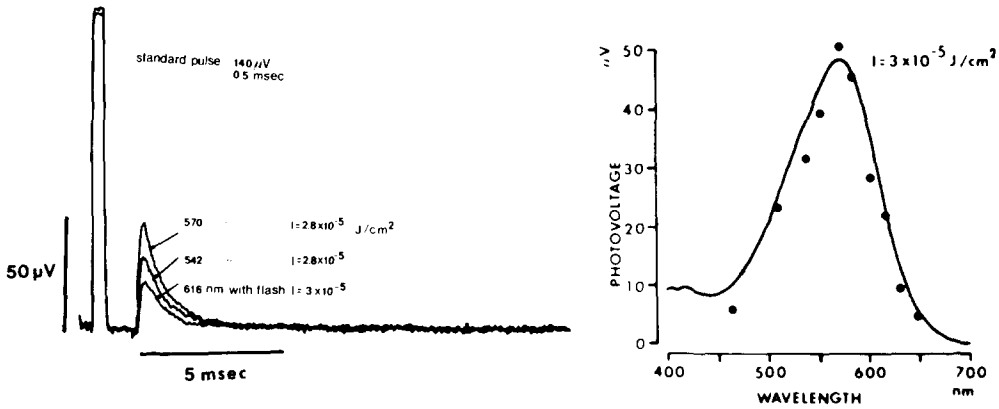

Fig. 3. Action spectrum of the BR_{570} photovoltage. Each tracing is the signal average of 64 photoresponses to actinic flashes presented every 20 s. A calibrating standard pulse was also signal averaged. Illustrated are photoresponses to actinic flashes of various wavelengths at a constant intensity. The graph illustrates the peak amplitude of photovoltages generated by actinic flashes of different wavelengths but identical intensity of $3 \cdot 10^{-5}$ J/cm^2. The continuous line is the absorption spectrum of BR_{570} scaled to give the best fit to the data points. Data shown were recorded from a sandwich cell consisting of 17 interface films.

does not exhibit any detectable latency with respect to the flash (see Fig. 4). Because the first photointermediate of BR_{570}, K_{590}, forms at room temperature on the time scale of 10^{-12} s [35], and since the actinic flash used in these experiments lasted approx. 10^{-3} s, the rate of photoexcitation of bacteriorhodopsin molecules in the sandwich cells should be limited simply by the rate of photon delivery by the actinic flash. The kinetics of BR_{570} photoexcitation (10^{-3} s time scale) is, therefore, slow compared with the electrical bandpass characteristics of the sandwich cells ($\tau < 10^{-6}$ s), and thus any voltage event

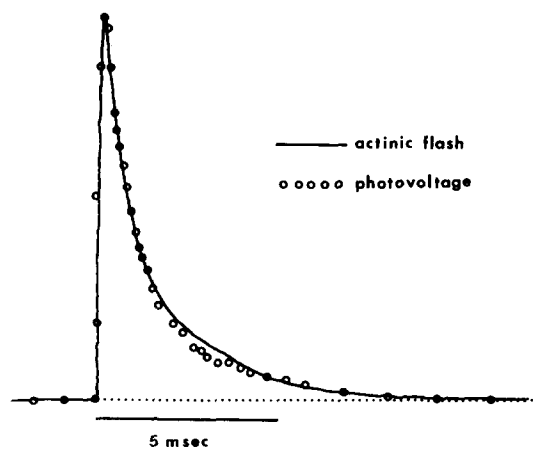

Fig. 4. Waveform of the BR_{570} photovoltage. The continuous line is the time course of the actinic flash as recorded through a photodiode (PIN 8LC, United Detector Technology, Santa Monica, Calif.). The open circles represent the waveform of the BR_{570} photovoltage generated by the same actinic flash and recorded simultaneously with the photodiode signal. The photovoltage is scaled to match peak amplitudes. The two waveforms closely match each other and no latency between them is detectable. Because of uncertainty in the signal averager, the latency between the two signals could be 60 μs but not more.

linked to the photoexcitation of BR_{570} would be expected to be undistorted by the cell assembly. Indeed, that the recorded photovoltages exhibit no latency and accurately follow the kinetics of the actinic flash indicates again that they are produced by a molecular event closely linked to the photoexcitation of BR_{570}.

The M_{412} and N_{520} photovoltage

To determine whether photovoltages could be generated by photoexcitation of intermediates in the bacteriorhodopsin photoreaction cycle in addition to BR_{570}, we took advantage of the fact that the kinetics of this cycle vary with relative humidity. At room temperature and physiological pH in aqueous suspensions of purple membrane, the M_{412} photointermediate forms with a time constant of about 30 μs and decays with a time constant of about 10 ms [9]. In contrast, in air-dried multilayer stacks of purple membrane, the half-time of decay of M_{412} is about 1 s *, whereas its half-time of formation is comparable to that in aqueous suspensions [16]. In the purple membrane sandwich cells, therefore, illumination with a 200 ms duration pulse of light should result in the formation of a photomixture containing BR_{570}, the M_{412} intermediate and possibly other slow intermediates which follow M_{412} in the photoreaction cycle. Each of these photointermediates might be distinguished by its characteristic visible absorption spectrum. Shown in Fig. 5 are typical photovoltages generated by flash illumination of constant intensity presented either alone or 2 ms after the end of a 200 ms duration conditioning pulse of light. Also illustrated is a complete action spectrum of the photovoltages generated under these conditions. In the absence of the conditioning pulse, the flash generates positive photovoltages throughout the visible range and the action spectrum matches well the absorption spectrum of BR_{570}. In contrast, following the conditioning pulse, smaller positive potentials are recorded in the red region of the spectrum and negative potentials in the blue region. Moreover, the action spectrum cannot be uniquely matched by the absorption spectrum of any one photointermediate. These results show that the conditioning pulse indeed produced a photomixture consisting of BR_{570} and several intermediates of the photoreaction cycle, and that photoexcitation of these intermediates generates transient photovoltages of both polarities.

To distinguish which intermediates, in addition to BR_{570}, generate photovoltages following the 200 ms conditioning pulse, we first attempted to subtract the contribution of BR_{570} photovoltage from the recorded signals. Because the time constant of formation of M_{412} and thus the decay of K_{590} and L_{550} in the purple membrane multilayer is fast, <100 μs [16], we assume that in addition to BR_{570} only the slow decay photointermediates M_{412}, N_{520} and O_{640} could contribute to the photovoltages generated 2 ms after the conditioning pulse. Furthermore, we have independently determined (see below) that O_{640} in these multilayers begins to form only about 250 ms following the

* This slowdown in the decay rate can be attributed to a drying effect, and not to an intrinsic change in the structure of bacteriorhodopsin, since the decay rate becomes comparable to that in aqueous suspension by simply immersing the multilayers in water [16]. R. Kornstein and B. Hess (personal communication) have confirmed this observation and have carefully characterized several kinetic components in the decay phase of the absorbance at 412 nm.

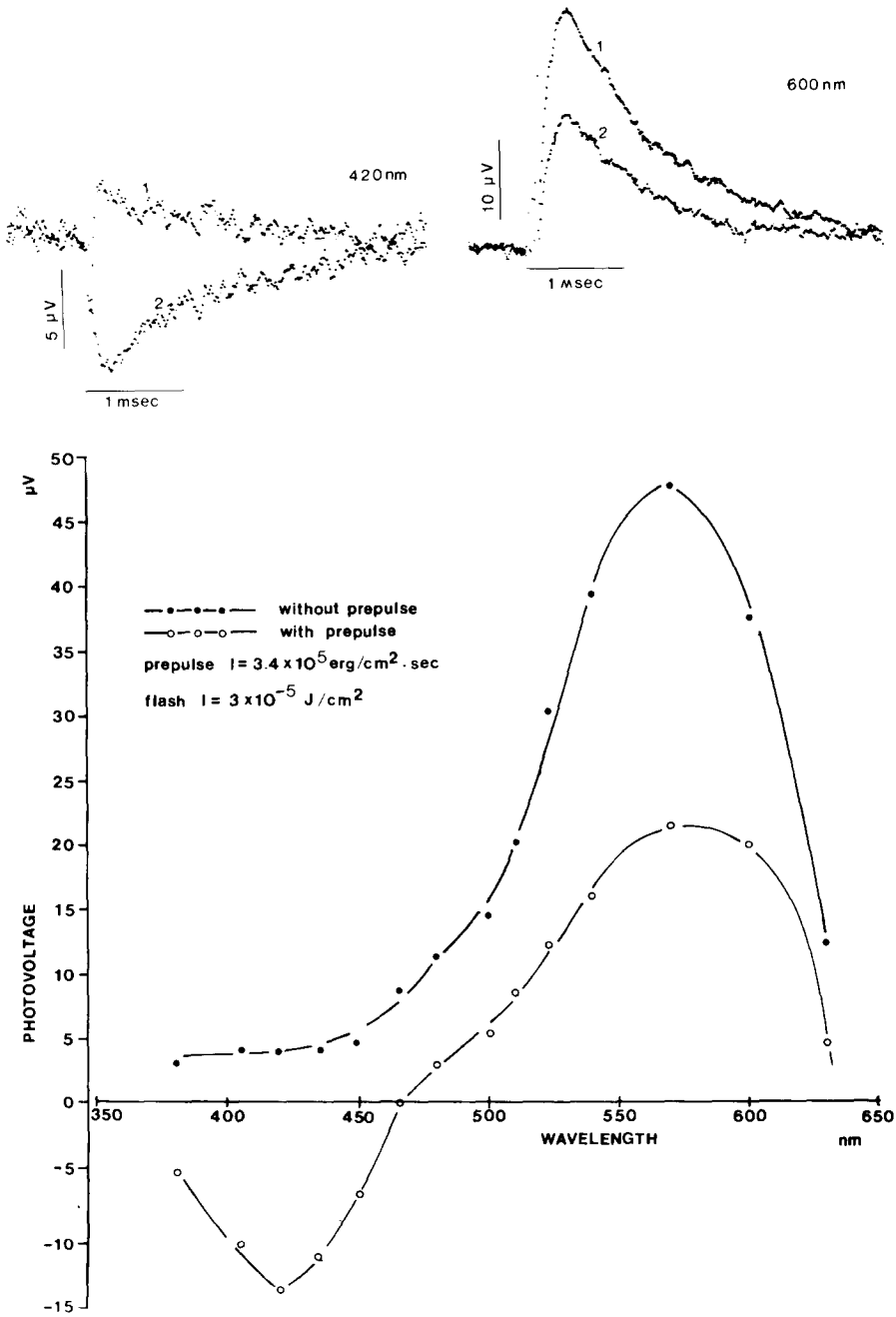

Fig. 5. Effects of a conditioning pulse on the action spectrum of the photovoltages. Each tracing is the signal average of 128 photoresponses to constant intensity actinic flashes of 420 nm or 600 nm presented either (1) alone or (2) 2 ms after a 200 ms duration conditioning pulse of light of wavelength longer than 540 nm (Corning Filer, OG-4). At 600 nm the photovoltage is reduced in amplitude. At 420 nm the photovoltage inverts polarity. The waveform of the photovoltage does not change. The graph illustrates the action spectrum of the peak amplitude of the photovoltages. Closed circles are data points measured in the absence of a conditioning pulse. Open circles are data points measured after the conditioning pulse. Each point is obtained from the signal average of 128 photosignals. The data shown were recorded from a cell consisting of 29 interface films.

end of the 200 ms conditioning pulse. Therefore, only BR_{570}, M_{412} and N_{520} can contribute to the photovoltages generated 2 ms after the conditioning pulse. Since neither M_{412} nor N_{520} absorb light at 600 nm [9,36], we assume that the response generated by the 600 nm actinic flash 2 ms after the conditioning pulse is a measurement of the fraction of BR_{570} molecules present in the photomixture. Following this reasoning, the contribution of the BR_{570} photovoltage to the photosignal generated after the conditioning pulse is found by simply multiplying each point in the action spectrum of BR_{570} (curve 1 in Fig. 5) by the ratio of the 600 nm photovoltages. Thus,

$$^{570}V_{\lambda}^{\text{cond}} = {}^{570}V_{\lambda}^{\text{dark}} \cdot \frac{V_{600}^{\text{cond}}}{V_{600}^{\text{dark}}}$$

where $^{570}V_{\lambda}^{\text{cond}}$ is the BR_{570} photovoltage at wavelength λ following the conditioning pulse and $^{570}V_{\lambda}^{\text{dark}}$ is the BR_{570} photovoltage at the same wavelength λ in the absence of the conditioning pulse.

The photovoltages generated by intermediates other than BR_{570}, V_{λ}, are obtained by subtracting the contribution of the BR_{570} photovoltage, $^{570}V_{\lambda}^{\text{cond}}$, from the voltage actually recorded, $^{\text{meas}}V_{\lambda}^{\text{cond}}$.

$$V_{\lambda} = {}^{\text{meas}}V_{\lambda}^{\text{cond}} - {}^{570}V_{\lambda}^{\text{cond}}$$

Fig. 6 illustrates the action spectrum obtained upon subtraction of the BR_{570} contribution from the data presented in Fig. 5. Negative potentials are recorded throughout the spectral range tested and two distinct broad bands are apparent, one which reaches peak near 410 nm and another which reaches peak near 520 nm. The points which reach peak near 410 nm match well the absorption spectrum of M_{412} as measured directly by Becher and Ebrey [36]. The points which peak near 520 nm match well the absorption spectrum of N_{520} as calculated by Lozier et al. [9]. Fig. 7 illustrates that the peak amplitude of the M_{412} photovoltage increases linearly with the flash stimulus intensity. Thus, the M_{412} photovoltage (see Fig. 5), like the BR_{570} photovoltage, exhibits no latency, has a waveform identical to that of the actinic flash at all intensities and its peak amplitude increases proportionately to light intensity. But, in contrast with the BR_{570} photovoltage, the M_{412} photovoltage (and also the N_{520} photovoltage) has a polarity such that the extracellular surface of the purple membrane becomes transiently negative with respect to the intracellular surface.

Because of the similar decay time constant of M_{412} and N_{520} in aqueous suspensions of purple membrane at room temperature and because of the closeness of their absorption maxima, the absorption spectrum of N_{520} has not yet been directly determined and its existence in the photoreaction cycle is still in question. Since we could distinguish photoelectric signals associated specifically with the M_{412} and N_{520} spectral intermediates, we attempted to use these photovoltages to distinguish the two intermediates kinetically. To do so we measured the peak amplitude of the M_{412} or N_{520} photovoltages generated by

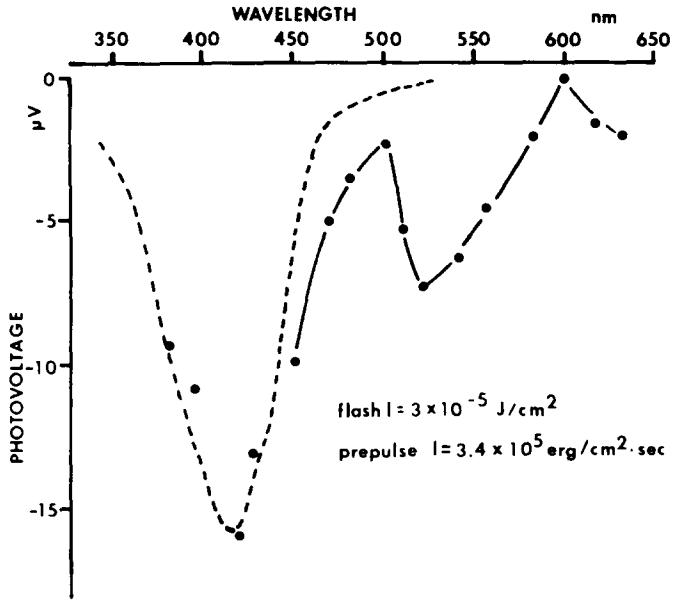

Fig. 6. The M_{412} and N_{520} photovoltages. Data points were obtained from Fig. 5 after subtracting the contribution of the BR_{570} photovoltage to the signals generated following a conditioning pulse (see text for method). Data points reach to a peak at two discrete wavelengths. The discontinuous line is the absorption spectrum of M_{412} as given by Becher and Ebrey [36] scaled to fit the points. The continuous line is drawn to join the data points and closely matches the absorption spectrum of N_{520} calculated by Lozier et al. [9]. The polarity of the voltage indicates that the extracellular surface of the purple membrane becomes transiently negative with respect to the intracellular surface.

actinic flashes of constant intensity presented either (1) 2 ms after a conditioning pulse of constant intensity but variable duration, or (2) at various time intervals after a 200 ms duration conditioning pulse of constant intensity. To carry out these measurements, the following protocol was used: The photo-

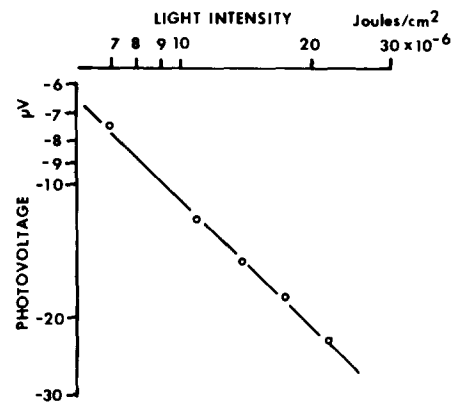

Fig. 7. The M_{412} photovoltage increases linearly with stimulus intensity. Actinic flashes of 420 and 600 nm and varying intensities were presented alone or 2 μs after a 200 ms conditioning pulse of light longer than 540 nm (Corning Glass, OG-4). From the average photovoltages thus produced the peak amplitude of the M_{412} photovoltage was calculated (see text for details). Data shown was obtained from a cell consisting of 29 layers.

voltage produced by 600 nm flashes was measured with and without the conditioning pulse under the conditions of pulse duration or time interval being tested. Photovoltages with either a 420 nm or 520 nm actinic flash were then generated with and without the conditioning pulse. Using the peak amplitude of all these photovoltages, the mathematical procedure outlined above was utilized to calculate the BR_{570} photovoltage contribution, and the net M_{412} and N_{520} photovoltages.

Fig. 8 illustrates the peak amplitude of the M_{412} and N_{520} photovoltages produced by constant intensity flashes presented 2 ms after conditioning pulse of between 50 and 200 ms duration. This procedure essentially measures the enrichment of the photomixture by M_{412} and N_{520} photointermediates for conditioning pulses of various durations. The M_{412} photovoltage reaches a maximum amplitude for conditioning pulses of about 100 ms duration. In contrast, the N_{520} photovoltage, develops more slowly and is detectable only following 150 ms duration pulses. These data indicate that indeed M_{412} and N_{520} are kinetically distinct intermediates and that N_{520} must follow M_{412} in the photocycle. The time constant of enrichment by M_{412} and N_{520} illustrated in Fig. 6 are determined by the relative humidity of the purple membrane sandwich cell. Experiments in other sandwich cell assemblies reveal similar kinetic differences between M_{412} and N_{520}, but the absolute value of the time constants varies from cell to cell. This is the result most likely of inadequate control on the extent of hydration of the multilayer cell. The data, nonetheless, confirm the independent identity of M_{412} and N_{520} and indicate that they can each independently produce transient voltages upon photoexcitation.

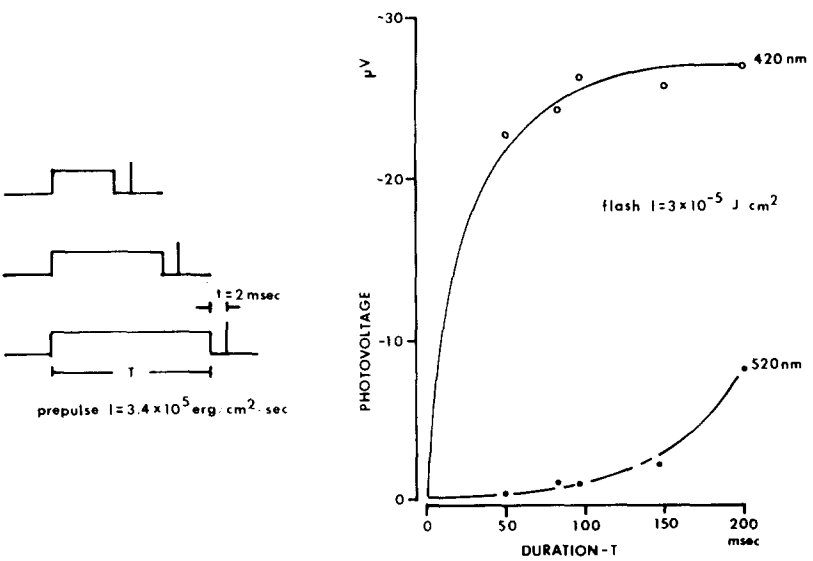

Fig. 8. Rate of enrichment in M_{412} and N_{520} in a photomixture. Variable duration conditioning pulses of light of wavelength longer than 540 nm were presented to a multilayer sandwich cell consisting of 27 layers. Before the conditioning pulse or 2 ms after the pulse, actinic flashes of constant intensity ($3 \cdot 10^{-5}$ J/cm^2) and 420, 520 and 600 nm were presented. The resulting photovoltages were averaged (128 responses) and their respective peak amplitudes were used to calculate the M_{412} and N_{520} photovoltages (see text for methods). The graph illustrates the peak amplitude of the M_{412} and N_{520} photovoltages generated for various durations of the conditioning pulse.

The O_{640} photovoltage

Fig. 9 illustrates the peak amplitudes of the M_{412} and N_{520} photovoltages produced by constant intensity flashes presented between 2 and 1500 ms after the end of a 200 ms duration conditioning pulse. This procedure essentially measures the rate of depletion of the M_{412} and N_{520} photointermediates from the photomixture produced by the conditioning pulse. Within the first 250 ms, while the M_{412} photovoltage is seen to decay, the N_{520} signal is still increasing. For time intervals longer than 250 ms, the M_{412} and N_{520} photovoltages can no longer be calculated because a signal due to photoexcitation of the O_{640} intermediate becomes detectable. The O_{640} intermediate absorbs significantly at 600 nm, and this then invalidates the assumption necessary to calculate the M_{412} and N_{520} photovoltages, i.e. that the 600 nm photovoltage is exclusively due to BR_{570}. Since only the O_{640} intermediate absorbs significantly at 690 nm [9], the photovoltage due to excitation of O_{640} was generated simply by presenting actinic flashes of 690 nm following the conditioning pulse. The O_{640} photovoltage has the same negative polarity as the M_{412} and N_{520} photovoltages. Again, it exhibits no detectable latency and its waveform is identical to that of the actinic flash. Thus, the photovoltages recorded across the purple membrane sandwich cells are consistent with the sequence of photointermediates M_{412} before N_{520} before O_{640}. However, whether the sequence is branched or linear cannot be uniquely determined from our data. In any event, it is clear that photoexcitation of BR_{570} and also of the intermediates M_{412}, N_{520} and O_{640} produces molecular events which generate transient voltages.

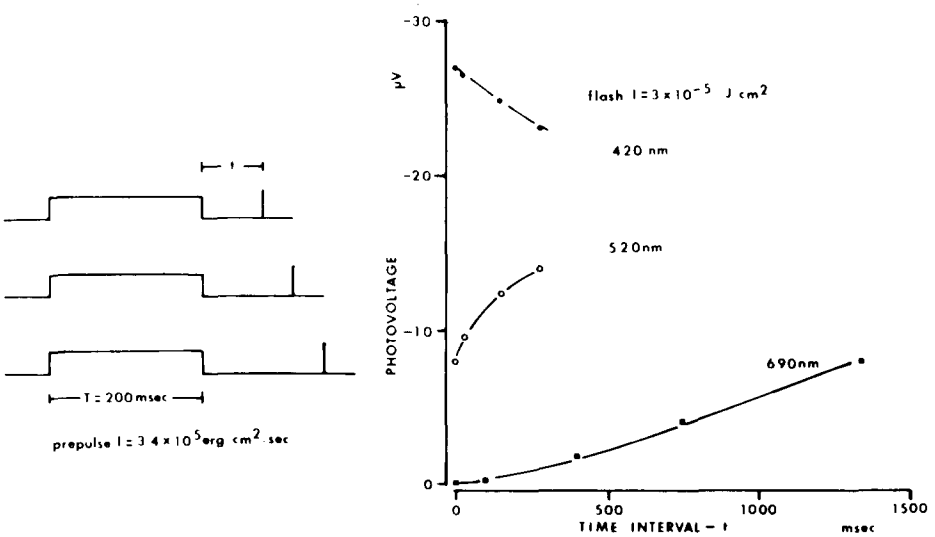

Fig. 9. Depletion of M_{412} and N_{520} in a photomixture. The O_{640} photovoltage. Photovoltages were generated by actinic flashes presented at various intervals after a conditioning pulse of 200 ms duration consisting of light of wavelength longer than 540 nm. The M_{412}, N_{520} and O_{640} photovoltages were calculated as described in the text. The graph illustrates the peak amplitude of the photovoltages generated by the same intensity flashes presented at various intervals after the conditioning pulse.

Discussion

In their light-adapted state, BR_{570}, bacteriorhodopsin molecules in the purple membrane proceed through a cyclic sequence of photochemical intermediates following illumination [9—12]. Only the formation of the first of these intermediates, K_{590}, requires light [9]. This intermediate decays thermally in the dark through a sequence of at least four other intermediates, L_{550}, M_{412}, N_{520} and O_{640}, before returning to the starting state. On the other hand, it is also possible to directly photoexcite some of these intermediates and have the pigment molecules return to the starting BR_{570} state. This photoreversibility has to date been demonstrated for the intermediates, K_{590} [9], M_{412} [36—38], and O_{640} (Lozier, R. and Ottolenghi, M., personal communication). With the use of an experimental cell consisting of films of highly oriented fragments of air-dried purple membrane and lipid stacked between two metal electrodes, we have shown above that photoexcitation of the BR_{570} state of bacteriorhodopsin and also of the intermediates M_{412}, N_{520} and O_{640} results in the generation of weak transient voltages. These photovoltages have been shown to exhibit no detectable latency, to be linearly proportional to incident light intensity and to exist in the absence of an electrolytic solution. Furthermore, the polarity of the photovoltages has been shown to depend only on the molecular species being photoexcited, whereas their waveforms depends on that of the actinic flash.

Other pigmented systems, most notably the rhodopsin-containing membranes of vertebrate and invertebrate photoreceptors also exhibit fast photovoltages with very similar features to those we have observed for the bacteriorhodopsin [39,40]. The photovoltages in the photoreceptor membranes, known as early receptor potentials, exhibit complex waveforms because they arise not only from the fast voltages generated by photoexcitation of the dark state of the pigment molecule, but also by transient voltages generated as the photointermediate states of rhodopsin decay thermally in the dark [39,41]. In addition, photoexcitation of each of the several photointermediates of rhodopsin can also generate independent transient voltages [41]. In the experiments with bacteriorhodopsin described here, we have only detected the transient voltage arising from the simultaneous photoexcitation of many BR_{570} molecules, but not that which might arise from the thermal return of the molecules to their starting state. On the other hand, we have found that photoexcitation of the molecules in the thermal return path: M_{412}, N_{520} and O_{640} all produce photovoltages of opposite polarity to that of the BR_{570} photovoltage. This suggests that perhaps by photosynchronizing the photointermediates in the return path we have detected electrically the molecular rearrangements of the pigment molecules as they return to their starting state. As pointed out above, several of the slow photointermediates are now known to be photoconvertible into BR_{570}.

The relatively long duration of the actinic flash used in the experiments reported here has not allowed us to resolve whether photointermediates formed prior to the M_{412} intermediate may also produce photovoltages. On the other hand, the fact that unique photovoltaic signals are associated with each of the slower intermediates in the photoreaction cycle and that the kinetics of this

cycle are slowed down in our experimental system has allowed us to show that the M_{412} and N_{520} photointermediates are indeed kinetically distinct and not two different absorption maxima of the same conformational state. Moreover, the formation and decay of M_{412} preceeds those of N_{520} under the conditions described here. R. Korenstein and B. Hess (personal communication) have found that O_{640} is detectable in dry samples of purple membrane only at a relative humidity above 90%. In contrast, we have detected an electrical signal by photoexcitation of O_{640} in our samples (55—70% humidity). The difference in these results may arise from the fact that the purple membrane fragments in our experimental cells are partially delipidated. Indeed, the existence of O_{640} in our samples has been determined spectrophotometrically (Bogomolni, R. and Hwang, S.-B., unpublished observations). Thus, photovoltaic signals have been used directly to complement spectrophotometric data (see also ref. 42). However, the limitations of this experimental approach must be clear: We have carried out a kinetic analysis of membranes under thermodynamic conditions which may well be different than those in aqueous suspensions.

These fast photoelectric events may arise from two possible physical mechanisms [43]: (1) A thermoelectric effect, in which light absorbed by bacteriorhodopsin heats one metal electrode more than the other and the resulting temperature gradients produce a flow of charge, and (2) molecular charge displacements within bacteriorhodopsin. In invertebrate photoreceptor membranes, a small thermoelectric contribution to fast photovoltages has been demonstrated by Hagins and McGaughy [40]. In the purple membrane sandwich cell described here, the thermoelectric effect, if any, must be small, since we were able to measure both positive and negative photovoltages as small as 1 μV, for constant intensity flashes depending exclusively on the photointermediate being stimulated, a result unexpected for simple thermoelectric effects. Also, control experiments demonstrated that illumination of sandwich cells formed exclusively from phospholipids did not exhibit photovoltages and that the size of the photovoltages recorded from purple membrane sandwich cells did not increase upon removal of the infrared-absorbing filters in the actinic beam. The observation that the fast photoelectric effects described here (1) demonstrate no detectable latency, (2) increase linearly with stimulus intensity, (3) change in polarity according to the photointermediate being excited, (4) occur in the absence of any electrolytic solutions, (5) occur in parallel with spectrophotometric changes, and (6) can be generated independently by several intermediates in the photoreaction cycle of bacteriorhodopsin all suggest that these responses arise from a net displacement of charge in the protein molecules as they respond to the absorption of photons.

Molecular charge displacements may arise from one of several possible events: Redistribution of net charge in the molecule, changes in the magnitude and/or orientation of permanent dipoles in the molecule, or transfer of charged particles (ions, protons or electrons) in or along the molecules. The precise molecular origin of the charge displacement in the BR_{570} state and the spectral intermediates of bacteriorhodopsin, of course remains to be established. Moreover, this molecular origin may be different for different intermediates. Evidence already exists to suggest that proton transfer steps occur within the bacteriorhodopsin molecule which do not lead directly to the release of free

protons into solution. For example, the Schiff base linkage between retinal and the protein, while protonated in the BR_{570} state, deprotonates in the time course of formation of the M_{412} intermediate [5,6], yet proton release from the protein occurs only after the formation of M_{412} [17]. Also, the Schiff base is inaccessible to small water-soluble reagents such as hydroxylamine and borohydride [44], suggesting that protons cannot be released directly from it into the aqueous phase. Kinetic isotope effects on the bacteriorhodopsin cycle have been reported [13—15], and Korenstein et al. [13,14] have used these data to propose that proton transfer steps occur in the pigment molecule associated with the formation and decay of intermediates, M_{412} and O_{640}. Bacteriorhodopsin consistst of seven closely packed α-helical segments oriented nearly perpendicular to the plane of the membrane [45] and Dunker and Zaleske [46] have proposed a molecular model for a highly efficient transfer of protons along interlocked α-helical proteins. Changes in the electrical dipole moment of rhodopsin have been reported to occur in parallel with the Metarhodopsin I to Metarhodopsin II transition, a transition which generates fast photovoltages [47]. Changes in the electrical dipole moment of bacteriorhodopsin may also occur in the experimental system described here.

With a simple experimental cell we have observed photovoltaic effects associated with actinic stimulation of the light-adapted form of bacteriorhodopsin and the photointermediates, M_{412}, N_{520} and O_{640}. These photovoltaic signals arise almost certainly from a net molecular charge displacement in the pigment molecule as it undergoes photochemical conversion in response to the absorption of light. Understanding of the events underlying this photovoltage may give us some insight into the molecular mechanism that pumps protons using light energy.

Acknowledgements

We thank G. Gold and D. Roof for helpful discussions. S.-B. Hwang was supported by a Sloan Foundation postdoctoral fellowship. J.I.K . is an Alfred P. Sloan Research fellow. Research was supported by N.I.H. grants EY 01586 and HL 06285.

References

1 Oesterhelt, D. and Stoeckenius, W. (1971) Nat. New Biol. 233, 149—152
2 Bridgen, J. and Walker, I.D. (1976) Biochemistry 15, 792—798
3 Oesterhelt, D. and Stoeckenius, W. (1973) Proc. Natl. Acad. Sci. U.S. 70, 2853—2857
4 Racker, E. and Stoeckenius, W. (1974) J. Biol. Chem. 249, 662—663
5 Lewis, A., Spoonhower, J., Bogomolni, R.A., Lozier, R.H. and Stoeckenius, W. (1974) Proc. Natl. Acad. Sci. U.S. 71, 4462—4466
6 Honig, B., Greenberg, A.D., Dinur, U. and Ebrey, T.G. (1976) Biochemistry 15, 4593—4599
7 Lewis, A., Fager, R.S. and Abrahamson, E.W. (1973) J. Raman Spectrosc. 1, 465—470
8 Honig, B. and Ebrey, T.G. (1974) Ann. Rev. Biophys. Bioeng. 3, 151—177
9 Lozier, R.H., Bogomolni, R.A. and Stoeckenius, W. (1975) Biophys. J. 15, 955—962
10 Dencher, N. and Wilms, M. (1975) Biophys. Struct. Mech. 1, 259—271
11 Kung, M., DeVault, D., Hess, B. and Oesterhelt, D. (1975) Biophys. J. 15, 907—910
12 Sherman, W.V., Slifkin, M.A. and Caplan, S.R. (1976) Biochim. Biophys. Acta 423, 238—248
13 Sherman, W.V., Korenstein, R. and Caplan, S.R. (1976) Biochim. Biophys. Acta 430, 454—458
14 Korenstein, R., Sherman, W.V. and Caplan, S.R. (1976) Biophys. Struct. Mech. 2, 267—276
15 Lozier, R.H. and Niederberger, W. (1977) Fed. Proc. 36, 1805—1809

16 Hwang, S.-B., Korenbrot, J.I. and Stoeckenius, W. (1977) J. Membrane Biol. 36, 115—136
17 Lozier, R.H., Niederberger, W., Bogomolni, R.A., Hwang, S.-B. and Stoeckenius, W. (1976) Biochim. Biophys. Acta 440, 545—556
18 Hwang, S.-B. and Stoeckenius, W. (1977) J. Membrane Biol. 33, 325—350
19 Hwang, S.-B., Korenbrot, J.I. and Stoeckenius, W. (1977) J. Membrane Biol. 36, 137—158
20 Bakker, E.P., Rottenberg, H. and Caplan, R. (1976) Biochim. Biophys. Acta 440, 557—572
21 Bogomolni, R. (1977) Fed. Proc. 36, 1833—1839
22 Renthal, R. and Lanyi, J.K. (1976) Biochemistry 15, 2136—2143
23 Racker, E. and Hinkle, P.C. (1974) J. Membrane Biol. 17, 181—188
24 Herrmann, T.R. and Rayfield, G.W. (1976) Biochim. Biophys. Acta 443, 623—628
25 Drachev, L.A., Frolov, V.N., Kaulen, A.D., Liberman, E.A., Ostrumov, S.A., Plakunova, V.G., Semenov, A.Y. and Skulachev, V.P. (1976) J. Biol. Chem. 251, 7059—7065
26 Trissl, H.W. and Montal, M. (1977) Nature 266, 655—657
27 Tang, C.W. and Albrecht, A.C. (1975) J. Chem. Phys. 62, 2139—2149
28 Lyons, L.E. and Newman, O.M.G. (1971) Aust. J. Chem. 24, 13—23
29 Oesterhelt, D. and Stoeckenius, W. (1974) in Methods in Enzymology, Biomembranes (Fleischer, S. and Estabrook, R., eds.), Vol. 31, pp. 667—678, Academic Press, New York
30 White, S.H. and Blessum, D.N. (1975) Rev. Sci. Instr. 46, 1462—1466
31 Mann, B. and Kuhn, H. (1971) J. Appl. Phys. 42, 4398—4405
32 Procarione, W.L. and Kauffman, J.W. (1974) Chem. Phys. Lipids 12, 251—260
33 Rosenberg, B. and Jendrasiak, G.L. (1968) Chem. Phys. Lipids 2, 47—54
34 Leslie, R.B., Chapman, D. and Hart, C.J. (1967) Biochim. Biophys. Acta 135, 797—811
35 Kaufmann, K.J., Rentzepis, P.M., Stoeckenius, W. and Lewis, A. (1976) Biochem. Biophys. Res. Commun. 68, 1109—1115
36 Becher, B. and Ebrey, T.G. (1977) Biophys. J. 17, 185—191
37 Hess, B. and Kuschmitz, D. (1977) FEBS Lett. 74, 20—24
38 Sperling, W., Carl, P., Rafferty, C.N. and Dencher, N.A. (1977) Biophys. Struct. Mech. 3, 79—94
39 Cone, R.A. and Pak, W.L. (1971) in Handbook of Sensory Physiology (Lowenstein, W.R., ed.), Vol. 1, pp. 345—382, Springer-Verlag, New York
40 Hagins, W.A. and McGaughy, R.E. (1967) Science 157, 813—816
41 Cone, R.A. (1967) Science 155, 1128—1131
42 Hwang, S.-B., Korenbrot, J.I. and Stoeckenius, W. (1977) in Membrane Bioenergetics (Packer, L. and Papageogiou, G., eds.), Elsevier, Amsterdam
43 Hagins, W.A. and Ruppel, H. (1971) Fed. Proc. 30, 64—68
44 Peters, J., Peters, R. and Stoeckenius, W. (1976) FEBS Lett. 61, 128—134
45 Henderson, R. and Unwin, P.N.T. (1975) Nature 257, 28—32
46 Dunker, A.K. and Zaleske, D.J. (1977) Biochem. J. 163, 45—57
47 Petersen, D.C. and Cone, R.A. (1975) Biophys. J. 15, 1181—1200